

Queuing models for abstracting interactions in Bacterial communities

Nicolò Michelusi, James Boedicker, Mohamed Y. El-Naggar and Urbashi Mitra

Abstract

Microbial communities play a significant role in bioremediation, plant growth, human and animal digestion, global elemental cycles including the carbon-cycle, and water treatment. They are also posed to be the engines of renewable energy via microbial fuel cells which can reverse the process of electrosynthesis. Microbial communication regulates many virulence mechanisms used by bacteria. Thus, it is of fundamental importance to understand interactions in microbial communities and to develop predictive tools that help control them, in order to aid the design of systems exploiting bacterial capabilities. This position paper explores how abstractions from communications, networking and information theory can play a role in understanding and modeling bacterial interactions. In particular, two forms of interactions in bacterial systems will be examined: *electron transfer* (ET) and *quorum sensing* (QS). While the diffusion of chemical signals has been heavily studied, ET occurring in living cells and its role in cell-cell interaction is less understood. Recent experimental observations open up new frontiers in the design of ET-based communication in microbial communities, which may coexist with the more well-known interaction strategies based on molecular diffusion. In QS, the concentration of certain signature chemical compounds emitted by the bacteria is used to estimate the bacterial population size, so as to activate collective behaviors. In this paper, new queueing models for ET and QS are proposed. These models are stochastic, and thus capture the inherent randomness exhibited by cell colonies in nature. It is shown that queueing models allow the characterization of the state of a single cell as a function of interactions with other cells and the environment, thus enabling the construction of an information theoretic framework, while being amenable to complexity reduction using methods based on statistical physics and wireless network design.

N. Michelusi and U. Mitra are with the Ming Hsieh Department of Electrical Engineering, University of Southern California, Los Angeles, USA; M. Y. El-Naggar and J. Boedicker are with the Department of Physics and Astronomy, University of Southern California, Los Angeles, USA; emails: {michelus, boedicke, mnaggar, ubli}@usc.edu

N. Michelusi and U. Mitra acknowledge support from one or all of these grants: ONR N00014-09-1-0700, CCF-0917343, CCF-1117896, CNS-1213128, AFOSR FA9550-12-1-0215, and DOT CA-26-7084-00. M. Y. El-Naggar acknowledge support from NASA Cooperative Agreement NNA13AA92A and grant DE-FG02-13ER16415 from the Division of Chemical Sciences, Geosciences, and Biosciences, Office of Basic Energy Sciences of the US Department of Energy.

I. INTRODUCTION

Bacteria constitute some of the earliest life forms on Earth, existing anywhere from four to three billion years ago [1]. Bacteria are unicellular organisms that lack a nucleus and rarely harbor membrane-bound organelles. While bacteria have certain elements in common (such as being unicellular), their numbers and variety are vast, with an aggregate biomass larger than that of all animals and plants combined [2]. Bacteria exist all over the planet, in and on living creatures, underground, and underwater. They can survive in Antarctic lakes and in hot springs, showing tremendous robustness and tenacity. It is theorized that bacteria enabled changes in the Earth's environment leading to atmospheric oxygen as well as being the precursors to more complex organisms. Microbial communities play a significant role in bioremediation, plant growth, human and animal digestion, global elemental cycles including the carbon-cycle, and water treatment [3]. Despite their simplicity as unicellular organisms, the operations and interactions of bacterial communities are not fully understood. Elucidating how bacteria interact with each other and with their environment is of fundamental importance in order to fully exploit their potential. To this end, it is important to develop realistic tools for the modeling and prediction of these systems.

In this position paper, we explore how abstractions from communications, networking and information theory can play a role in understanding and modeling bacterial interactions. In particular, we shall examine two forms of interactions in bacterial systems: *electron transfer* [4], [5] and *quorum sensing* [6]–[8].

a) Electron Transfer (ET): While chemical and molecular diffusion are widely investigated [9], [10], ET is emerging as an exciting strategy by which bacteria exchange nutrients and potentially information. ET is fundamental to cellular respiration: each cell relies on a continuous flow of electrons from an electron donor (ED) to an electron acceptor (EA) through the cell's electron transport chain (ETC) to produce energy in the form of the molecule adenosine triphosphate (ATP), and to sustain its vital operations and functions. This strategy, known as *oxidative phosphorylation*, is employed by all respiratory microorganisms. While the importance of biological ET is well-known for individual cells, the past decade has also brought about remarkable discoveries of multicellular microbial communities that transfer electrons between cells and across much larger length scales than previously thought [11], spanning from molecular

assemblies known as *bacterial nanowires*, to entire macroscopic architectures, such as biofilms and multicellular bacterial cables [4], [5]. ET has been observed in nature [5] and in colonies cultured in the laboratory [12]. This multicellular interaction is typically initiated by a lack of either ED or EA, which in turn triggers gene expression. The overall goal in these extreme conditions is for the colony to survive despite deprivation, by relaying electrons from the ED to the EA in order to support the ETC in each cell. The survival of the whole system relies on this division of labor, with the intermediate cells operating as *relays* of electrons to coordinate this collective response to the spatial separation of ED and EA.

These observations open up new frontiers in the modeling and design of ET-based communication in microbial communities, which may coexist with the more well-known interaction strategies based on molecular diffusion, and motivate us to examine the capacity of multicellular ET, in order to understand how many electrons can be maximally transferred. Such questions are of fundamental interest in the design and optimization of microbial fuel cells (see Sec. I-B). A logical question to ask is whether classical approaches to cascaded channels are suitable for the study of bacterial cables, which are indeed *multi-hopped* networks [13]. Communication over cascades has been persistently studied since the 1950's starting with early works on the capacity of such systems (see, *e.g.*, [14]–[17]). A straightforward cut-set bound analysis [18] shows that the capacity of such a system is achieved by a decode-and-forward strategy. However, in microbial systems, there is a stronger interaction between the bacteria, due to the coupling of the electron signal with the energetic state of the cells via the ETC. Thus, alternative strategies for analysis and optimization must be undertaken,¹ which take into account the specificity of the interactions between cells in a bacterial cable. In turn, it is important to understand how to design capacity-achieving signaling schemes over bacterial cables, which exploit these specific interactions, as a preliminary step towards optimizing fuel cell design. In Sec. II, we present a stochastic queuing model of ET for a single cell, which links ET to the energetic state of the cell (*e.g.*, ATP concentration). This model abstracts the detailed working of a single cell by using interconnected queues to model signal interactions. In Sec. III, we show how the proposed single-cell model can be extended to larger communities (*e.g.*, cables, biofilms), by allowing ET between neighboring cells. In Sec. III-A, based on such a model, we perform a capacity analysis

¹Relay systems employing decode and forward for molecular diffusion based communication systems are considered in [19].

for a bacterial cable, and discuss the design of signaling schemes.

b) Quorum Sensing (QS): As previously noted, biological systems are known to communicate by diffusing chemical signals in the surrounding medium [9], [10]. In QS, the concentration of certain signature chemical compounds emitted by the bacteria is used to estimate the bacterial population size, so as to activate collective behaviors. However, this simplistic explanation does not fully capture the complexity and variety of QS related processes. In this paper, we provide a model for QS, informed by our ET work, that will enable more sophisticated study and analyses. While QS is based on the emission, diffusion and detection of these chemical signatures across the environment in which the cell colony lives, it differs from recent work endeavoring to design transceiver algorithms based on molecular diffusion channels. This recent explosion of research has focused on the modeling and analysis of such channels (see, *e.g.*, [20]–[24]) as well as on information theoretic analyses (see, *e.g.*, [25]–[29]) to determine their capacity.

The focus of these works is the design of models and algorithms for engineered systems for future nanomachines to act as transmitters and receivers. Herein, instead, we attempt to understand natural systems and their optimization via the control of environmental conditions. Rather than looking at the characteristics of the diffusion channel, we consider the system (the cell colony and the surrounding environment) as a whole, and attempt to model the dynamic interactions between cells and of the cells with the environment. We abstract the diffusion channel by considering a queueing model to represent it in terms of concentration of signals. As will be seen in our model depicted in Fig. 6, QS does not fit well into traditional multi-terminal frameworks such as the multiple access channel [30]–[33], the broadcast channel [34], [35] or two-way communication [30]. In fact, recent work examining capacity questions relating to QS have considered the binding of molecules and multicellular processes with molecular diffusion [27], [36]. The models adopted therein do not take the dynamics of the binding processes into consideration as we do here.

A. Prior Art on Mathematical Modeling of Bacterial Populations

The modeling of natural populations such as swarms (motile bacteria, swimming fish, flying birds, or migratory herds of animals) has been consistently studied over the years. *Microscopic models* consider individual behaviors via dynamical equations often modeling individuals as point particles [37]–[39]. These models have precision, but become much more complex as the

interactions are finely modeled and do not scale well as the population size increases. To combat such issues, the computational approach of simulating a large number of agents with prescribed interaction rules has also been considered [37], [40], [41]. These studies duplicate experimental results well, but do not lead to design methodologies or optimization strategies as the underlying operations are not considered. In contrast, *macroscopic models* model biological swarm dynamics via advection-diffusion-reaction partial differential equations (PDEs) [39], [42]–[46]. The PDEs are used to describe the evolution of the probability distribution of group sizes or fraction of individuals with specific characteristics (*e.g.*, motion orientation [47]). These approaches also suffer from computational complexity, often relying on numerical solvers, and do not have an eye towards optimization and control.

From an information theoretic perspective, there have been ongoing efforts to examine how entropy and mutual information² can provide insights into experimental data [49]–[51]; however these works do not endeavor to model the underlying processes, but rather compute empirical information theoretic measures based on experimental data. Another key distinction is a lack of an explicit modeling of the dynamics of the constituent systems.

Our modeling approach differs from these mathematical models on the following aspects: 1) We propose an accurate queueing approach to characterize the state of a single cell as a function of interactions with other cells and the environment. Thus, not only this approach can be used to describe the metabolic state of a cell, but it also enables the construction of an information theoretic framework; 2) our proposed models are inherently stochastic (rather than deterministic), and thus capture the inherent randomness exhibited by cell colonies in nature; 3) finally, they are amenable to complexity reduction, *e.g.*, using methods based on statistical physics [52] or wireless network design [53]. We show an example of application of these principles to the capacity analysis of bacterial cables in Sec. III-A.

B. Applications

The proposed queueing models serve as powerful predictive tools, which will aid the design of systems exploiting bacterial capabilities. We highlight two relevant applications.

²See [48] for a review of the application of information theory to biology.

1) *Microbial Fuel Cells (MFCs)*: Renewable energy technologies based on bioelectrochemical systems (BES) are now attracting tens of millions of dollars in government and industry funding [11]. MFCs and the essentially reverse process of microbial electrosynthesis are well known BES-based technologies; both use microorganisms to either generate electricity or biofuels in a sustainable way [54]. MFCs are constructed with microbes that oxidize diverse organic fuels, including waste products and raw sewage, while routing the resulting electrons to large-area electrodes where they are harvested as electricity [55]. Certain bacterial strains (*e.g.*, *Shewanella oneidensis* [55], [56]) are of particular interest for MFCs as they can attach to electrodes and transfer electrons without *mediators* which are often toxic, especially in the high concentrations needed to overcome their diffusion.

The challenge to realizing MFCs is understanding the cooperative and anti-cooperative behaviors of collections of bacteria. Ideally, as the number of bacteria increases, the amount of current generated should increase as well. However, this is not always observed in many experimental scenarios [57]. We posit that the cell-cell interactions necessitated by a multicellular (*i.e.* biofilm) lifestyle, including ET across and through the biofilms themselves, can limit device performance. In other words, the biofilm’s energy output cannot be casually gleaned from what we know about the mechanisms relevant to individual or “disconnected” microbes. Optimization of biofilms, and multicellular performance in general, requires sophisticated models and predictive tools that account for the electronic and nutrient fluxes within whole communities. In this paper, we propose queuing models to serve this purpose.

2) *Suppression of Infections*: QS processes have been of significant interest since first observed in *Vibrio harveyi* [8]. The discovery of QS in *Pseudomonas aeruginosa*, a human pathogen associated with cystic fibrosis and burn wound infections, demonstrates the medical implications of QS regulation [58], [59]. In *Pseudomonas aeruginosa* infections, QS plays an important role in activating many critical virulence pathways [60], [61]. The genes regulated by QS enable the bacteria to mount a successful attack or evade the body’s defenses. In these cases, QS activation is not desirable; in fact, blocking QS activation may help to prevent or treat microbial-associated diseases [62]. As bacteria build resistance to antibiotics, reducing virulence through QS inhibition may be more effective in mitigating disease versus eradicating the bacteria [63]. Naturally occurring compounds and enzymes exist which can inhibit QS [62], [64]. However, the complexity of signaling interactions within complex communities of microbes points to the need

for a more quantitative understanding of QS regulation. Because many different types of bacteria use a similar set of signals, and many signals work in conjunction with other autoinducers within the same cell, the potential outcomes of QS manipulation are not obvious. The combination of predictive model development with quantitative experiments to parametrize and test models are essential to develop successful strategies for virulence reduction.

This paper is organized as follows. In Secs. II and III, we propose a model of ET for a single cell and a bacterial cable, respectively, and present some capacity results. In Sec. IV, we present a model of QS in a homogeneous bacterial community. In Sec. V, we present some simulation results and, in Sec. VI, we discuss extensions of the proposed QS model. Finally, in Sec. VII, we conclude the paper.

II. SINGLE CELL MODEL OF ELECTRON TRANSFER

In this section, we propose a queuing model of ET in a single cell. We will extend this model to interconnections of cells in a bacterial cable in Sec. III. The cell is modeled as a system with an input electron flow coming either from the ED via molecular diffusion, or from a neighboring cell via ET, and an output flow of electrons leaving either toward the EA via molecular diffusion, or toward the next cell in the cable via ET (Fig. 1). Inside the cell, the conventional pathway of electron flow, enabled by the presence of the ED and the EA, is as follows (see the numbers in Fig. 1): ED molecules permeate inside the cell via molecular diffusion (1), resulting in reactions that produce electron-containing carriers (*e.g.*, NADH) (2), which are collected in the *internal electron carrier pool* (IECP). The electron carriers diffusively transfer electrons to the ETC, which are then discarded by either a soluble and internalized EA (*e.g.*, molecular Oxygen) or are transferred through the periplasm to the outer membrane and deposited on an extracellular EA (3). The electron flow through the ETC results in the production of a proton concentration gradient (proton motive force, [65]) across the inner membrane of the cell (4), which is utilized by the inner membrane protein *ATP synthase* to produce ATP, collected in the *ATP pool* and later used by the cell as an energy source (5).

A. Stochastic cell model

In this section, we present our proposed cell model. Each cell incorporates four pools (see Fig. 1), each with an associated state, as a function of time t :

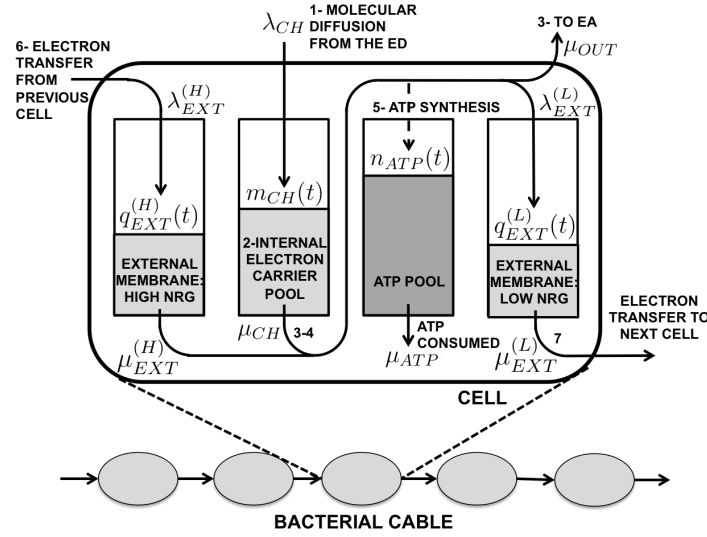


Fig. 1. Stochastic model of electron transfer within a bacterial cable.

- 1) The *IECP*, which contains the electron carrier molecules (e.g., NADH) produced as a result of ED diffusion throughout the cell membrane and chemical processes occurring inside the cell, with state $m_{CH}(t) \in \mathcal{M}_{CH} \equiv \{0, 1, \dots, M_{CH}\}$ representing the number of electrons³ bonded to electron carriers in the IECP, where M_{CH} is the *electro-chemical storage capacity*;
- 2) The *ATP pool*, containing the ATP molecules produced via ETC, with state $n_{ATP}(t) \in \mathcal{N}_{ATP} \equiv \{0, 1, \dots, N_{ATP}\}$, representing the number of ATP molecules within the cell, where N_{ATP} is the ATP capacity of the cell;
- 3) The *external membrane pool*, which involves the extracellular respiratory pathway of the cell in the outer membrane. This is further divided into two parts: a) a *High energy*⁴ *external membrane* (HEEM), which contains high energy electrons coming from previous cells in the cable; and b) a *Low energy external membrane* (LEEM), which collects low energy electrons from the ETC, before they are transferred to a neighboring cell. We denote the number of electrons in the HEEM and LEEM as $q_{EXT}^{(H)}(t) \in \mathcal{Q}_{EXT}^{(H)} \equiv \{0, 1, \dots, Q_{EXT}^{(H)}\}$, and $q_{EXT}^{(L)}(t) \in \mathcal{Q}_{EXT}^{(L)} \equiv \{0, 1, \dots, Q_{EXT}^{(L)}\}$, where $Q_{EXT}^{(H)}$ and $Q_{EXT}^{(L)}$ are the electron “storage capacities” of the HEEM and LEEM, respectively.

³While in the following analysis we assume that one queuing “unit” corresponds to one electron, this can be generalized to the case where one “unit” corresponds to N_E electrons.

⁴Note that the terms *high* and *low* referred to the energy of electrons are used here only in relative terms, *i.e.*, relative to the redox potential at the cell surface. In bacterial cables, the redox potential slowly decreases along the cable, thus inducing a net electron flow.

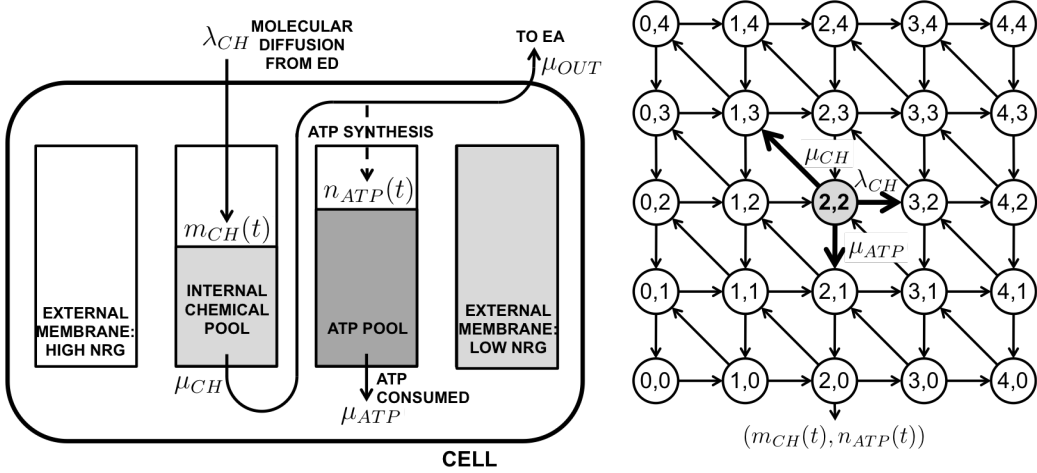


Fig. 2. Stochastic model for an isolated cell after the transient phase, and Markov chain with the corresponding transitions, for the case where $M_{CH} = N_{ATP} = 4$. The transition rates from state $(2, 2)$ are also depicted.

The *internal state* of the cell at time t is thus

$$\mathbf{s}_I(t) = \left(m_{CH}(t), n_{ATP}(t), q_{EXT}^{(L)}(t), q_{EXT}^{(H)}(t) \right). \quad (1)$$

The behavior of the cell is also influenced by the concentration of the ED and the EA in the surrounding medium. Therefore, we also define the *external state* as $\mathbf{s}_E(t) = (\sigma_D(t), \sigma_A(t))$, where $\sigma_D(t)$ and $\sigma_A(t)$ are, respectively, the external concentration of the ED and the EA.

Each pool in this model has a corresponding inflow and outflow of electrons, each modeled as a Poisson process with rate function of the internal and external state of the cell, as represented in Fig. 1.

B. Model Validation for an Isolated Cell

In the case of an isolated cell, multicellular ET does not occur, hence $\mu_{EXT}^{(L)} = \lambda_{EXT}^{(H)} = 0$. Therefore, after a transient phase during which the LEEM and HEEM get emptied and filled, respectively, the cell's state and the corresponding Markov chain and state transitions are as depicted in Fig. 2. In [66], we have validated this model based on experimental data available in [67], using the following parametric model for the rates, inspired by biological constraints

(e.g., Fick's law of diffusion [68]):

$$\begin{aligned}\lambda_{CH}(\mathbf{s}_I(t); \mathbf{s}_E(t)) &= \rho \left(1 - \frac{m_{CH}(t)}{M_{CH}}\right) \sigma_D(t), \\ \mu_{OUT}(\mathbf{s}_I(t); \mathbf{s}_E(t)) &= \mu_{CH}(\mathbf{s}_I(t); \mathbf{s}_E(t)) = \zeta \left(1 - \frac{n_{ATP}(t)}{N_{AXP}}\right) \sigma_A(t), \\ \mu_{ATP}(\mathbf{s}_I(t); \mathbf{s}_E(t)) &= \beta \sigma_D(t),\end{aligned}\tag{2}$$

where $\rho, \zeta, \beta \in \mathbb{R}_+$ are parameters, estimated via curve fitting, and $M_{CH} = N_{AXP} = 20$.

Initially, cells are starved and the ED concentration is 0. At time $t = 80\text{s}$, glucose is added to the cell culture. Afterwards, the ED concentration profile decreases in a staircase fashion from $\sigma_D(t) = 30[\text{mM}]$ glucose at time $t = 80\text{s}$, to $\sigma_D(t) = 0[\text{mM}]$ at time $t = 1300\text{s}$, and $\sigma_D(t) = 0[\text{mM}]$ for $t < 80\text{s}$, whereas the EA concentration (molecular Oxygen) is constant throughout the experiment, and sufficient to sustain reduction ($\sigma_A(t) = 1, \forall t$) [67]. We have designed a parameter estimation algorithm based on maximum likelihood principles, outlined in [66], to fit the parameter vector $\mathbf{x} = [\rho, \zeta, \beta]$ to the experimental data in [67]. The estimated parameters are given by

$$\begin{cases} \hat{\rho} = 2 \times 10^5 \text{ electrons/mM/s}, \\ \hat{\zeta} = 4.2 \times 10^5 \text{ electrons/s}, & \hat{\beta} = 0.92 \times 10^5 \text{ ATP molecules/mM/s}. \end{cases}$$

where mM refers to the glucose ED concentration.

Fig. 3 plots the ATP time-series, related to the cell culture, and the expected predicted values based on our proposed stochastic model. We observe a good fit of the prediction curves to the experimental ones. In accordance with [67], the addition of the ED to the suspension of starved cells triggers an increase in ATP and NADH production as well as ATP consumption, as observed experimentally and predicted by our model.

III. TOWARDS A MODEL OF BACTERIAL CABLES

In multicellular structures, such as bacterial cables, an additional pathway of electron flow may co-exist, termed *intercellular electron transfer* (IET), which involves a transfer of electrons between neighboring cells, as opposed to molecules (ED and EA) diffusing through the cell membrane. In this case, one or both of the ED and the EA are replaced by neighboring cells in a network of inter-connected cells. This cooperative strategy creates a multicellular ETC that utilizes IET to distribute electrons throughout an entire bacterial network. Electrons originate

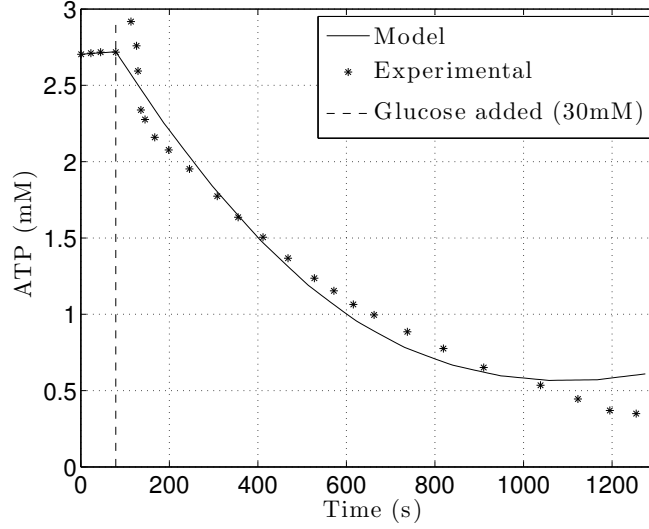


Fig. 3. Prediction of expected ATP level over time (in mM) and experimental time-series.

from the ED localized on one end of the network and terminate to the EA on the other end. The collective electron transport through this network provides energy for all cells involved to sustain their vital operations.

Since typical values for transfer rates between electron carriers (*e.g.* outer-membrane cytochromes) on the cell exterior are relatively high [13], we assume that $\mu_{EXT}^{(L)} = \lambda_{EXT}^{(H)} = \infty$ when two cells are connected, so that any electron collected in the LEEM is instantaneously transferred to the HEEM of the neighboring cell in the cable. Therefore, the LEEM and HEEM pools of two neighboring cells can be joined into a common pool for IET. The *internal state* of cell i at time t is thus

$$\mathbf{s}_I^{(i)}(t) = \left(m_{CH}^{(i)}(t), n_{ATP}^{(i)}(t), q_{EXT}^{(L)(i)}(t), q_{EXT}^{(H)(i)}(t) \right), \quad (3)$$

and its *external state* is $\mathbf{s}_E^{(i)}(t) = (\sigma_D^{(i)}(t), \sigma_A^{(i)}(t))$.

The state of the cable of length N is denoted as $\mathbf{s}(t) = (\mathbf{s}^{(1)}(t), \mathbf{s}^{(2)}(t), \dots, \mathbf{s}^{(N)}(t))$, where $\mathbf{s}^{(i)}(t) = (\mathbf{s}_I^{(i)}(t), \mathbf{s}_E^{(i)}(t))$.

The internal state $\mathbf{s}_I^{(i)}(t)$ is time-varying and stochastic, and evolves as a consequence of electro/chemical reactions occurring within the cell, chemical diffusion through the cell membrane, and IET from the neighboring cell $i - 1$ to cell i , and then to the neighboring cell $i + 1$. The evolution of $\mathbf{s}_I^{(i)}(t)$ is also influenced by the external state $\mathbf{s}_E^{(i)}(t)$ experienced by the cell. Let

$\mathbf{s}_I^{(i)}(t) = (m_{CH}, n_{ATP}, q_{EXT}^{(L)}, q_{EXT}^{(H)})$ be the state of the i th cell at time t , and t^+ be the time instant immediately following t . We define the following processes which affect the evolution of $\mathbf{s}_I^{(i)}(t)$, all of which, for analytical tractability, are modeled as Poisson processes with, possibly, state-dependent rates, expressed in [electrons/s] (see Fig. 1):

- *ED diffusion* through the membrane, joining the IECP with rate $\lambda_{CH}(\mathbf{s}_I^{(i)}(t); \mathbf{s}_E^{(i)}(t))$. The state becomes $\mathbf{s}_I^{(i)}(t^+) = (m_{CH} + 1, n_{ATP}, q_{EXT}^{(L)}, q_{EXT}^{(H)})$;
- *IET* from the neighboring cell $i - 1$, joining the HEEM with rate $\lambda_{EXT}^{(L)}(\mathbf{s}_I^{(i-1)}(t); \mathbf{s}_E^{(i-1)}(t))$ (in fact, owing to the high transfer rate approximation, the electron joining the LEEM of cell $i - 1$ is immediately transferred to the HEEM of cell i), resulting in $\mathbf{s}_I^{(i)}(t^+) = (m_{CH}, n_{ATP}, q_{EXT}^{(L)}, q_{EXT}^{(H)} + 1)$;
- *Conventional ATP synthesis*: this process involves the transfer of one electron from the IECP to the internal membrane with rate $\mu_{CH}(\mathbf{s}_I^{(i)}(t); \mathbf{s}_E^{(i)}(t))$, resulting in the synthesis of one unit of ATP. The electron then leaves the internal membrane and either follows the *aerobic pathway* (i.e., it is captured by an EA), with rate $\mu_{OUT}(\mathbf{s}_I^{(i)}(t); \mathbf{s}_E^{(i)}(t))$, resulting in $\mathbf{s}_I^{(i)}(t^+) = (m_{CH} - 1, n_{ATP} + 1, q_{EXT}^{(L)}, q_{EXT}^{(H)})$, or the *anaerobic* one (i.e., it is collected in the LEEM, also the HEEM of cell $i + 1$), with rate $\lambda_{EXT}(\mathbf{s}_I^{(i)}(t); \mathbf{s}_E^{(i)}(t))$, so that $\mathbf{s}_I^{(i)}(t^+) = (m_{CH} - 1, n_{ATP} + 1, q_{EXT}^{(L)} + 1, q_{EXT}^{(H)})$;
- *Unconventional ATP synthesis*: this process involves the transfer of one electron from the HEEM to the internal membrane to synthesize one unit of ATP, with rate $\mu_{EXT}^{(H)}(\mathbf{s}_I^{(i)}(t); \mathbf{s}_E^{(i)}(t))$. Afterwards, the electron follows either the aerobic pathway with rate $\mu_{OUT}(\mathbf{s}_I^{(i)}(t); \mathbf{s}_E^{(i)}(t))$, resulting in $\mathbf{s}_I^{(i)}(t^+) = (m_{CH}, n_{ATP} + 1, q_{EXT}^{(L)}, q_{EXT}^{(H)} - 1)$; or the anaerobic one with rate $\lambda_{EXT}^{(L)}(\mathbf{s}_I^{(i)}(t); \mathbf{s}_E^{(i)}(t))$, so that $\mathbf{s}_I^{(i)}(t^+) = (m_{CH}, n_{ATP} + 1, q_{EXT}^{(L)} + 1, q_{EXT}^{(H)} - 1)$;
- *ATP consumption*, with rate $\mu_{ATP}(\mathbf{s}_I^{(i)}(t); \mathbf{s}_E^{(i)}(t))$, resulting in $\mathbf{s}_I^{(i)}(t^+) = (m_{CH}, n_{ATP} - 1, q_{EXT}^{(L)}, q_{EXT}^{(H)})$.

A. Information capacity of bacterial cables

In [69], building on our recent queuing theoretic model of bacterial cables [66], we have studied the information capacity of bacterial cables. By treating the bacterial cable as a communication medium, its capacity represents the maximum amount of information that can be transferred through the cable, and thus sets the limit on the rate at which cells can communicate via ET.

Importantly, as shown in [69] and in the following analysis, communication over a bacterial cable entails two conflicting factors: 1) achieving high instantaneous information rate; 2) inducing the bacterial cable to operate in information efficient states. In fact, the input electron signal

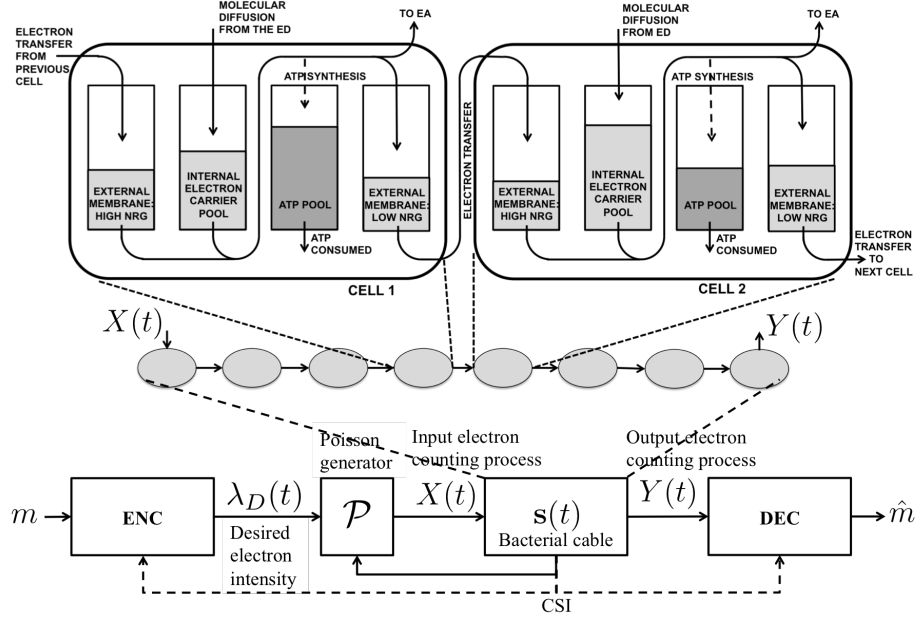


Fig. 4. Communication system over a bacterial cable. "ENC"=encoder, "DEC"=decoder.

affects the energetic state of the cells along the cable via the ETC, and thus affects their ability to relay electrons and to transfer information. Thus, our analysis underlines the importance of channel state information at the encoder, which enables *adaptation* of the input signal to the state of the cable, in order to optimize this trade-off.

1) *Queuing model*: The model [66] presumes that the channel state is given by the interconnection of the state of each cell in the cable, leading to high dimensionality. As shown in Fig. 4, the bacterial cable contains N cells. Letting \mathcal{S}_{cell} be the state space of the internal state of each cell, then the overall state space of the cable is $\mathcal{S} \equiv \mathcal{S}_{cell}^N$, which grows exponentially with the bacterial cable length N . Indeed, one of the advantages of our proposed queuing model is its amenability to complexity reduction. Herein, we propose an abstraction of [66] by treating the bacterial cable as a black box, which captures only the *global* effects on the electron transfer efficiency of the cable, resulting from the *local* interactions and cells' dynamics presumed by [66].⁵ Specifically, we let $E(t)$ be the number of electrons carried in the cable, *i.e.*, the sum of the number of electrons carried in the external membrane of each cell, which

⁵Importantly, research on ET over bacterial cables [5], [11] is relatively new and ongoing, and new models may prevail as new experimental evidence becomes available and the fundamental mechanisms better understood (*e.g.*, [70]). Our model, by abstracting the detailed cell-cell interactions and cells' dynamics within the cable, does not preclude other physical models that describe the fundamental mechanisms of bacterial cables and the metabolism of the cells involved. New models can be thus included by appropriate selection of the clogging function $\alpha(\cdot)$, as well as leakage and interference functions (not present in the model considered in this paper, but included in [69]).

participate in the ETC to produce ATP for the cell.⁶ The state space for this approximate model is $\mathcal{E} \equiv \{0, 1, \dots, E_{\max}\}$, where E_{\max} is the electron carrying capacity of the bacterial cable. Letting $E_{\max}^{(cell)}$ be the electron carrying capacity of a single cell, we have that $E_{\max} = N \cdot E_{\max}^{(cell)}$, which scales linearly with the cable length, rather than exponentially.

The rationale behind this approximate model is as follows: when $E(t)$ is large, the large number of electrons in the cable can sustain a large ATP production rate, so that the ATP pools of the cells are full and the cable is clogged. When this happens, the electron relaying capability of the bacterial cable is reduced, so that only a portion of the input electrons can be relayed. On the other hand, when $E(t)$ is small, a weak electron flow occurs along the cable, so that the ATP pools are almost empty, the cells are energy-deprived, and the cable can thus sustain a large input electron flow to recharge the ATP pools. We thus define the *clogging function* $\alpha(E(t)) \in [0, 1]$, which represents the fraction of electrons which can be relayed at the input of the cable. This model is in contrast to classical relay channels over cascades, where the performance is dictated by the worst link rather than by a clogging function [18].

The communication system includes an encoder, which maps the message $m \in \{1, 2, \dots, M\}$ to a *desired electron intensity* $\lambda(t)$, taking binary values $\lambda(t) \in \{\lambda_{\min}, \lambda_{\max}\}$, $t \in [0, T]$,⁷ where T is the codeword duration, and $\lambda_{\min} > 0$ and $\lambda_{\max} > \lambda_{\min}$ are, respectively, the minimum and maximum electron intensities allowed into the cable.

The channel state $E(t)$ evolves in a stochastic fashion as a result of electrons randomly entering and exiting the cable. Electrons enter the bacterial cable following a Poisson process with rate $\lambda_{in}(t) = \alpha(E(t))\lambda(t)$, resulting in the state $E(t)$ to increase by one unit, where $\alpha(i) \in [0, 1]$ is the clogging function and $\lambda(t)$ is the desired electron intensity, which is part of our design. Electrons exit the cable following a Poisson process with rate $\mu(E(t))$, resulting in the state $E(t)$ to decrease by one unit. In general, $\alpha(i)$ is a non-increasing function of i , with $\alpha(E_{\max})=0$, $\alpha(0)=1$, $\alpha(i)>0, \forall i < E_{\max}$. In fact, the larger the amount of electrons carried by the cable $E(t)$, the more severe the ATP saturation and electron clogging along the cable, and thus the smaller $\alpha(E(t))$.

⁶Our model in [69] studies a general model with leakage and interference. Herein, for simplicity, we assume no leakage nor interference.

⁷Herein, we restrict the input signal to take binary values, since this choice is optimal [69].

2) *Capacity analysis*: Using results on the capacity of finite-state Markov channels [71], we have proved that the capacity of bacterial cables is given by

$$\mathcal{I} = \max_{\bar{\lambda}: \mathcal{E} \mapsto [\lambda_{\min}, \lambda_{\max}]} \sum_{i=0}^{E_{\max}} \pi_{\bar{\lambda}}(i) I(\bar{\lambda}(i); i), \quad (4)$$

where

- $\bar{\lambda}(i)$ is the average desired input electron intensity in state $E(t) = i$, defined as

$$\bar{\lambda}(i) \triangleq \mathbb{E}[\lambda(t) | E(t) = i], \quad (5)$$

which is the goal of our design;

- $I(\bar{\lambda}(i); i)$ is the *instantaneous mutual information rate* in state $E(t) = i$ with expected desired input electron intensity $\bar{\lambda}(i)$, given by

$$I(x; i) \triangleq \alpha(i) \left[x \log_2 \left(\frac{\lambda_{\max}}{x} \right) + \frac{\lambda_{\max} - x}{\lambda_{\max} - \lambda_{\min}} \lambda_{\min} \log_2 \left(\frac{\lambda_{\min}}{\lambda_{\max}} \right) \right]; \quad (6)$$

- $\pi_{\bar{\lambda}}(i)$ is the asymptotic steady-state distribution of the bacterial cable, induced by the desired input electron intensity $\bar{\lambda}(\cdot)$, given by

$$\pi_{\bar{\lambda}}(i) = \prod_{k=0}^{i-1} \frac{\alpha(k) \bar{\lambda}(k)}{\mu(k+1)} \pi_{\bar{\lambda}}(0), \quad (7)$$

where $\pi_{\bar{\lambda}}(0)$ is obtained via normalization ($\sum_i \pi_{\bar{\lambda}}(i) = 1$).

The capacity optimization problem in Eq. (4) is a Markov decision process [72], with state $E(t)$, action $\bar{\lambda}(i)$ in state $E(t) = i$, which generates the binary intensity signal, and reward function $I(\bar{\lambda}(i); i)$ in state $E(t) = i$, and can thus be solved efficiently using standard optimization algorithms, *e.g.*, policy iteration (see [72]). The following trade-off arises: 1) the optimal input signal should, on the one hand, achieve high instantaneous information rate, *i.e.*, it should maximize $I(\bar{\lambda}(E(t)); E(t))$ at each time instant t ; 2) on the other hand, it should induce an "optimal" steady-state distribution of the cable, such that those states characterized by less severe clogging and where the transmission of information is more favorable are visited more frequently. These two goals are in tension. In fact, the instantaneous information rate is maximum in states with large clogging state $\alpha(i) \simeq 1$, *i.e.*, when $E(t)$ is small and the bacterial cable is deprived of electrons. Visits to these states are achieved more frequently by choosing $\lambda(t) = \lambda_{\min}$ with

probability one. However, under a deterministic input distribution the information rate is zero.

3) *Myopic signaling*: While the optimal signaling $\bar{\lambda}^*(i)$ balances this tension by giving up part of the instantaneous transfer rate in favor of a better steady-state distribution in the future, *i.e.*, states characterized by large clogging state $\alpha(E(t)) \simeq 1$ where a larger instantaneous mutual information rate can be achieved, the *myopic* signal greedily maximizes the instantaneous information rate, without considering its impact on the steady-state distribution of the cable. This is defined as

$$\bar{\lambda}_{MP}(i) \triangleq \arg \max_{x \in [\lambda_{\min}, \lambda_{\max}]} I(x; i) = \frac{\lambda_{\max}}{e} \left(\frac{\lambda_{\min}}{\lambda_{\max}} \right)^{-\frac{\lambda_{\min}}{\lambda_{\max} - \lambda_{\min}}}, \quad \forall i \in \mathcal{E}, \quad (8)$$

and is constant with respect to the cable state $E(t) = i$, so that it does not require channel state information at the encoder. Importantly, the myopic signal neglects the steady-state behavior of the cable, and thus it tends to quickly recharge the ATP reserves of the cells, resulting in severe clogging of the cable. Thus, the myopic signaling may induce frequent visits to states characterized by small clogging state $\alpha(E(t)) \simeq 0$, *i.e.*, when $E(t)$ approaches E_{\max} .

Indeed, in [69] we have shown that any input distribution $\bar{\lambda}(i)$ larger than the myopic one $\bar{\lambda}_{MP}(i)$ is deleterious to the capacity for the following two reasons: 1) a lower instantaneous mutual information rate is achieved, compared to $\bar{\lambda}_{MP}(i)$ (by definition of the myopic distribution, which maximizes $I(x; i)$); 2) faster recharges of electrons within the cable are induced, resulting in frequent clogging of the cable, where the instantaneous information rate is small.

4) *Numerical results*: We consider a cable with electron capacity $E_{\max} = 1000$. The clogging state $\alpha(i)$ and output rate $\mu(i)$ are given by⁸

$$\alpha(i) = \chi(i < E_{\max}) \left[1 - (1 - \alpha_{\min}) \frac{i}{E_{\max}} \right], \quad \mu(i) = 0.6 + 0.8 \frac{i}{E_{\max}}. \quad (9)$$

In Fig. 5.a, we note that the achievable information rate increases with α_{\min} under both the optimal signaling (OPT) and the myopic signaling (MP). This is because, as α_{\min} increases, both $\alpha(i)$ and the instantaneous information rate $I(x; i)$ increase as well (see Eqs. (9) and (6)). Intuitively, the larger $\alpha(i)$, the better the ability of the bacterial cable to transport electrons.

OPT outperforms MP by $\sim 9\%$ for small values of α_{\min} . In fact, clogging is severe when

⁸The specific choices of $\alpha(i)$ and $\mu(i)$ have been discussed with Prof. M. Y. El-Naggar and S. Pirbadian, Department of Physics and Astronomy, University of Southern California, Los Angeles, USA.

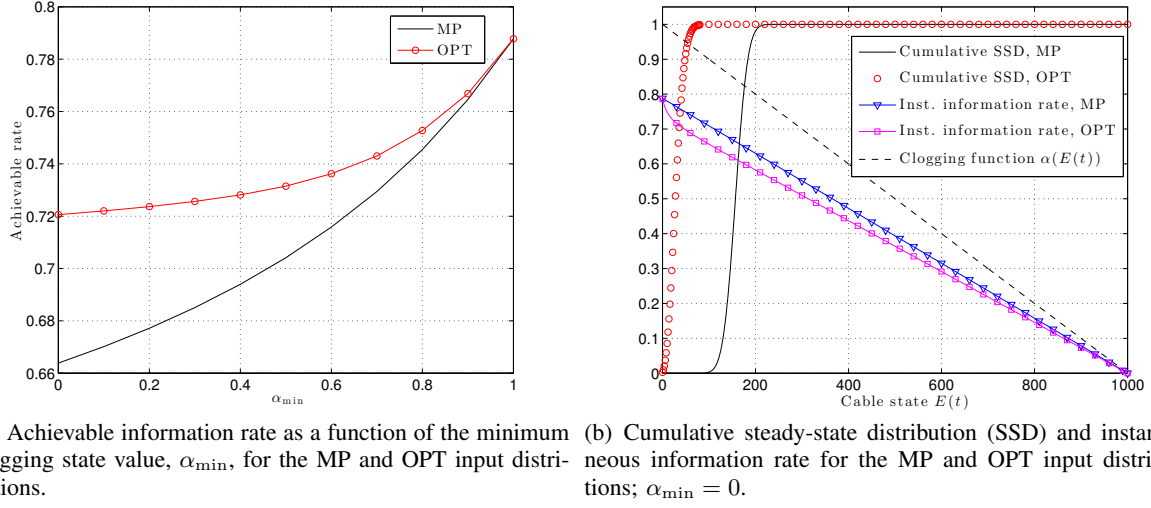


Fig. 5. Capacity of bacterial cables

the cable state approaches the maximum value E_{\max} . Therefore, in order to achieve high instantaneous information rate, the state of the cable $E(t)$ should be kept small. MP greedily maximizes the instantaneous information rate, but this action results in an unfavorable steady-state distribution (see Fig. 5.b), such that the cable is often in large queue states $E(t) \simeq E_{\max}$, where clogging is severe and most electrons are dropped at the cable input. On the other hand, OPT gives up some instantaneous information rate in order to favor the occupancy of low queue states, where $\alpha(i)$ approaches one and the transfer of information is maximum. The performance degradation of MP with respect to OPT is less severe when $\alpha_{\min} \rightarrow 1$. In fact, in this case the instantaneous information rate $I(x; i)$ is the same in all states (except E_{\max} , where $\alpha(E_{\max}) = 0$ and $I(x; E_{\max}) = 0$), so that optimizing the steady-state distribution of the cable becomes unimportant.

IV. TOWARDS A MODEL OF QUORUM SENSING (QS) IN A HOMOGENEOUS CELL COLONY

In the previous section, we proposed a queuing model of ET over bacterial cables, and we have shown how complexity reduction can be achieved by a compact state space representation $E(t)$, which represents the number of electrons carried in the cable, and by defining a *clogging function* $\alpha(i)$ over such state space. Similarly, in this section, we propose a queuing model for the simplest QS signaling, for the case of a homogeneous cell colony which uses a single autoinducer-receptor pair, depicted in Figs. 6.a-b. This is the case, for instance, for *Chromobacter*

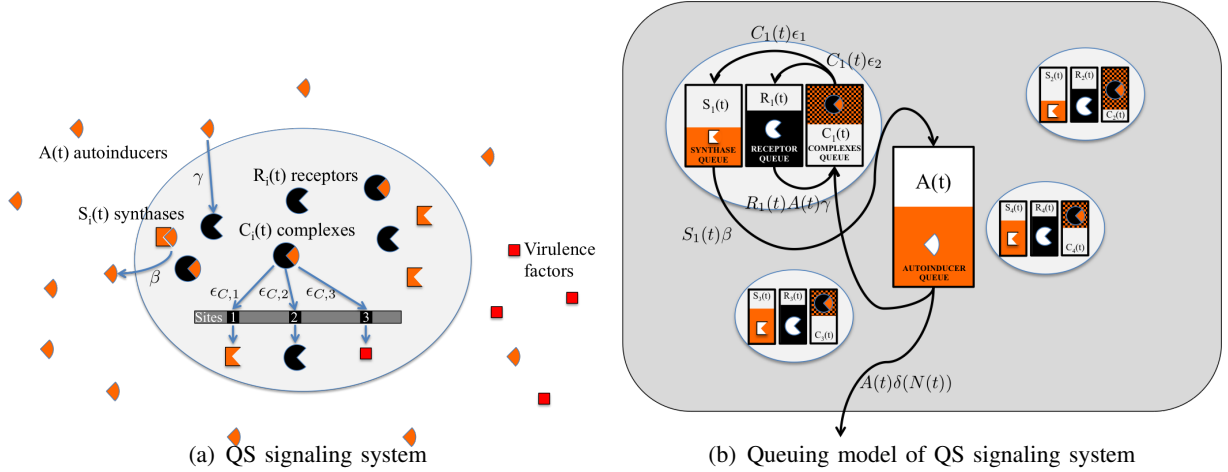


Fig. 6. QS signaling system and queuing model

violaceum [73]. Similarly to the queuing model of ET, this model can then be used as a baseline for further model reduction techniques.

We consider a colony composed of $N(t)$ identical cells at time t . We assume these cells can duplicate, but do not die. In fact, only a small fraction of cells under favorable growth conditions are dead ($< 0.01\%$) [74], therefore cell death has a negligible influence on the dynamics of QS. We model cell duplication for each cell as a Poisson process with intensity $\rho(n)$, depending on the cell population size $N(t) = n$, i.e., each cell duplicates once every $1/\rho(n)$ hours, on average. Therefore, $N(t)$ is a counting process with time-varying intensity $N(t)\rho(N(t))$. One model of $\rho(n)$ is the *logistic growth model* $\rho(n) = \rho_{\max} (1 - n/N_{\max})$, where ρ_{\max} is the maximum growth rate and N_{\max} is the maximum population size. This model presumes that growth slows down as the population increases, until $N(t) = N_{\max}$ when growth stops. We denote the volume of a single cell as ϕ_{cell} , so that the total cell volume of a colony of $N(t) = n$ cells is $V_{\text{cell}}(n) = n\phi_{\text{cell}}$, and the total volume occupied by the colony (cell volume and extracellular environment) as $V_{\text{tot}}(n)$. Here we consider both closed systems, with a fixed total volume $V_{\text{tot}}(n) = \text{constant}$, and open systems, in which the volume changes with the number of cells,

$$V_{\text{tot}}(n) = n\phi_{\text{ex}}, \quad (10)$$

where ϕ_{ex} is the volume occupied by each cell (cell volume and extracellular environment).

The QS signaling system is characterized by different signals, represented in Fig. 6.a: *au-*

autoinducer molecules, produced by the *synthases* within each cell and released in the environment; *receptors*, located within each cell, which bind with the autoinducer molecules to form *autoinducer-receptor complexes*; these complexes then bind to the active DNA sites to produce further synthases, receptors and virulence factors. The dynamics of each of these signals and their interaction are characterized herein.

A. Environment state

Let $A(t)$ be the number of autoinducer molecules in the system. Thus, the concentration of autoinducers in the volume occupied by the colony is $\eta_A(t) \triangleq A(t)/V_{tot}(N(t))$. The dynamics of $A(t)$ over time is affected by autoinducer production, degradation, receptor binding, and leakage. Leakage accounts for the autoinducer molecules that leak out of the volume before being captured by the cells. We assume that the larger the colony, the smaller the leakage. In fact, the larger the colony of cells, the higher the likelihood that these molecules are detected before they diffuse out of the system. Additionally, autoinducer molecules may chemically degrade thus becoming inactive. We thus let $\delta_A(n)$ be the rate of leakage and degradation for each autoinducer molecule as a function of the number of cells $N(t) = n$, where $\delta_A(n) \geq \delta_A(n+1), \forall n \geq 1$. One choice of $\delta_A(n)$ is

$$\delta_A(n) = \xi_D + \frac{\xi_{L,1}}{1 + \xi_{L,2}(n-1)}, \quad (11)$$

where ξ_D is the degradation rate of each autoinducer molecule, $\xi_{L,1}$ is the leakage rate when only one cell is present, and $\xi_{L,2}$ is the rate of decay of the leakage as the colony size increases. This model presumes that, when the number of cells doubles, the leakage rate is approximately halved. Given that there are $A(t)$ autoinducer molecules in the system, the overall leakage rate is $A(t)\delta_A(N(t))$.

Remark 1. Both $\xi_{L,1}$ and $\xi_{L,2}$ depend on the diffusion properties of the medium and the spatial distribution of the cells [75]. For a closed system, where no leakage occurs, we have that $\xi_{L,1} = 0$, hence $\delta_A(n) = \xi_D, \forall n$. However, (11) may not capture all possible scenarios. Other scenarios can be accommodated by an appropriate selection of the leakage rate $\delta_A(n)$ (possibly, different from (11)).

B. Cell state

Each cell is described by three state variables, as represented in Fig. 6.b. For cell i , we let $R_i(t)$ be the number of unbound receptors at time t , and $C_i(t)$ be the number of autoinducer-receptor complexes within the cell. Each cell uses a protein called *synthase* to synthesize autoinducers. In turn, these autoinducers are released outside the cell through its membrane. We let $S_i(t)$ be the number of synthases present within cell i at time t . The state of cell i is thus given by the tuple $(R_i(t), C_i(t), S_i(t))$ at time t . No leakage of receptors, complexes or synthases outside of the cell occurs.

Each of the $C_i(t)$ autoinducer-receptor complexes randomly binds to active sites in the DNA sequence, resulting in specific gene expression (see Fig. 6.a). We assume three active binding sites: 1) the first site contains the code to produce *synthases*, resulting in the increase of $S_i(t)$ by one unit; 2) the second site contains the code to produce receptors, resulting in the increase of $R_i(t)$ by one unit; 3) the third site contains the code to produce the virulence factor of the QS signaling system.

Remark 2. It is worth noting that, while in the case of *Chromobacter violaceum* the receptor and the synthase are made from distinct DNA binding sites, in some cases both compounds are made from the same DNA binding site [76]. This scenario can be incorporated by letting the first site contain the code to synthesize *both* synthases and receptors, resulting in the increase of *both* $S_i(t)$ and $R_i(t)$ by one unit. Additionally, individual binding events may lead to the production of multiple synthases or receptors [77]. This scenario can be included by defining a random number of synthases or receptors produced at each binding event, with a given probability distribution.

After the gene is expressed, the autoinducer-receptor complex unbinds from the DNA site. We assume that the binding-unbinding process is instantaneous, *i.e.*, we neglect the amount of time that the complex occupies the DNA site. We model the process of autoinducer-receptor complexes binding to the DNA sites as Poisson processes, whose intensities depend on the affinity of the complex to a specific site. Thus, we let $\epsilon_{C,j}, j \in \{1, 2, 3\}$ be the binding rate of each complex to site j (see Fig. 6.a). Additionally, gene expression occurs even in the absence of complexes, at basal rate $\epsilon_{0,j}, j \in \{1, 2, 3\}$. Therefore, since there are $C_i(t)$ autoinducer-receptor complexes within cell i , the gene located in site j is expressed with overall rate $\epsilon_{0,j} + C_i(t)\epsilon_{C,j}$.

C. State dynamics

$N(t)$ *increases* over time due to cell growth; $A(t)$ *increases* over time as the synthases located within each cell produce autoinducers, and *decreases* over time as a result of autoinducers binding to receptors, leakage and degradation (Sec. IV-A); $R_i(t)$ *increases* over time as the cell synthesizes receptors, and *decreases* over time as a result of autoinducers binding to receptors and receptor degradation; similarly, $C_i(t)$ *increases* over time as the unbound receptors bind to the autoinducer signal in the environment, and decreases over time as a result of degradation and complex unbinding; finally, $S_i(t)$ increases over time as the cell produces synthases, and decreases over time as a result of degradation.

We let

$$R_{\text{TOT}}(t) \triangleq \sum_{i=1}^{N(t)} R_i(t), \quad C_{\text{TOT}}(t) \triangleq \sum_{i=1}^{N(t)} C_i(t), \quad S_{\text{TOT}}(t) \triangleq \sum_{i=1}^{N(t)} S_i(t), \quad (12)$$

be the total amount of receptors, complexes and synthases of the cell colony, and

$$\eta_R(t) \triangleq \frac{R_{\text{TOT}}(t)}{V_{\text{cell}}(N(t))}, \quad \eta_C(t) \triangleq \frac{C_{\text{TOT}}(t)}{V_{\text{cell}}(N(t))}, \quad \eta_S(t) \triangleq \frac{S_{\text{TOT}}(t)}{V_{\text{cell}}(N(t))}, \quad (13)$$

be their concentrations, respectively.⁹ There are several processes that affect the dynamics of $(N(t), A(t), R_{\text{TOT}}(t), C_{\text{TOT}}(t), S_{\text{TOT}}(t))$, as detailed below.

a) Cell duplication: Cell duplication occurs with rate $\rho(N(t))$ for each cell, so that the cell population $N(t)$ increases by one unit with rate $\rho(N(t))N(t)$. When one cell duplicates, its content is split randomly among the two cells. Therefore, if $(R_i(t), C_i(t), S_i(t))$ is the state of cell i before its duplication, after the duplication (at time instant t^+) there are two cells with state $(R_i^{(1)}(t^+), C_i^{(1)}(t^+), S_i^{(1)}(t^+))$ and $(R_i^{(2)}(t^+), C_i^{(2)}(t^+), S_i^{(2)}(t^+))$, respectively, where $R_i^{(1)}(t^+) + R_i^{(2)}(t^+) = R_i(t)$, $C_i^{(1)}(t^+) + C_i^{(2)}(t^+) = C_i(t)$, and $S_i^{(1)}(t^+) + S_i^{(2)}(t^+) = S_i(t)$, with probability distribution

$$\begin{aligned} & \mathbb{P} \left((R_i^{(1)}(t^+), C_i^{(1)}(t^+), S_i^{(1)}(t^+)) = (r, c, s) | R_i(t), C_i(t), S_i(t) \right) \\ &= \binom{R_i(t)}{r} \binom{C_i(t)}{c} \binom{S_i(t)}{s} 2^{-R_i(t)-C_i(t)-S_i(t)}. \end{aligned} \quad (14)$$

⁹Note that receptors, complexes and synthases are located inside the cell rather than in the extracellular environment, therefore their concentrations are calculated with respect to the total cell volume $V_{\text{cell}}(N(t))$.

b) One autoinducer is created: Each synthase produces autoinducers with rate β . Since there are $S_{\text{TOT}}(t)$ synthases, the cell colony produces autoinducers with rate $\beta S_{\text{TOT}}(t)$, resulting in the increase of $A(t)$ by one unit.

c) One autoinducer leaks or degrades: Each autoinducer leaks or degrades with rate $\delta_A(N(t))$. Therefore, autoinducer leakage and degradation occurs with rate $\delta_A(N(t))A(t)$, resulting in the decrease of $A(t)$ by one unit.

d) One receptor is created: One receptor is created whenever one complex binds to the second active DNA site. This occurs with rate $N(t)\epsilon_{0,2} + C_{\text{TOT}}(t)\epsilon_{C,2}$ across the whole cell colony, resulting in the increase of $R_{\text{TOT}}(t)$ by one unit.

e) One receptor degrades: Each receptor degrades with rate δ_R . Therefore, receptor degradation occurs with rate $\delta_R R_{\text{TOT}}(t)$, resulting in the decrease of $R_{\text{TOT}}(t)$ by one unit.

f) One complex is created: Typically, binding of autoinducers to receptors to form autoinducer-receptor complexes does not occur until a threshold concentration of autoinducers is achieved [78]. We let this threshold be $\eta_{A,\text{th}}$. Thus, if $\eta_A(t) < \eta_{A,\text{th}}$, then no binding of autoinducers to receptors occurs. When the threshold is exceeded, *i.e.*, $\eta_A(t) \geq \eta_{A,\text{th}}$, then the binding of autoinducers to receptors is a Poisson process with intensity γ [per unit of autoinducer and receptor concentrations, per unit volume, per hour]. Since the concentrations of autoinducers and free receptors is $\eta_A(t)$ and $\eta_R(t)$, respectively, and the total cellular volume where these reactions occur is $V_{\text{cell}}(N(t)) = N(t)\phi_{\text{cell}}$, complexes form with rate

$$\gamma \eta_A(t) \eta_R(t) \chi(\eta_A(t) \geq \eta_{A,\text{th}}) V_{\text{cell}}(N(t)) = \gamma \frac{A(t) R_{\text{TOT}}(t)}{V_{\text{tot}}(N(t))} \chi(A(t) \geq \eta_{A,\text{th}} V_{\text{tot}}(N(t))), \quad (15)$$

resulting in the decrease of $A(t)$ and $R_{\text{TOT}}(t)$ by one unit,¹⁰ and in the increase of $C_{\text{TOT}}(t)$ by one unit.

g) One complex degrades: Each autoinducer-receptor complex degrades with rate δ_C . Therefore, autoinducer-receptor complex degradation occurs with rate $\delta_C C_{\text{TOT}}(t)$, resulting in the decrease of $C_{\text{TOT}}(t)$ by one unit.

h) One complex unbinds: Each complex may randomly unbind, and the constituent autoinducer and receptor molecules become active again. This event occurs with rate v_C for each

¹⁰In this paper, for simplicity, we assume that one receptor binds to one autoinducer to form one complex. However, in most systems, two receptors bind an autoinducer.

complex. Therefore, unbinding of complexes occurs with rate $v_C C_{\text{TOT}}(t)$, resulting in the decrease of $C_{\text{TOT}}(t)$ by one unit and in the increase of $A(t)$ and $R_{\text{TOT}}(t)$ by one unit.

i) One synthase is created: One synthase is created whenever one complex binds to the first active DNA site. This occurs with rate $N(t)\epsilon_{0,1} + C_{\text{TOT}}(t)\epsilon_{C,1}$ across the whole cell colony, resulting in the increase of $S_{\text{TOT}}(t)$ by one unit.

j) One synthase degrades: Each synthase degrades with rate δ_S . Therefore, synthase degradation occurs with rate $\delta_S S_{\text{TOT}}(t)$, resulting in the decrease of $S_{\text{TOT}}(t)$ by one unit.

k) Virulence factor expression: Finally, the gene located in site 3 is expressed with intensity $\epsilon_{0,3} + C_i(t)\epsilon_{C,3}$ in cell i , resulting in the overall expression with intensity $N(t)\epsilon_{0,3} + C_{\text{TOT}}(t)\epsilon_{C,3}$ over the whole cell colony.

D. State representation and state space reduction

Let $\mathbf{R}(t) = [R_1(t), R_2(t), \dots, R_{N(t)}(t)]$ be the vector of receptor concentrations, $\mathbf{C}(t) = [C_1(t), C_2(t), \dots, C_{N(t)}(t)]$ be the vector of autoinducer-receptor complexes concentrations, and $\mathbf{S}(t) = [S_1(t), S_2(t), \dots, S_{N(t)}(t)]$ be the vector of synthase concentrations. These vectors have time-varying length $N(t)$, due to cell duplication. Then, the state of the system at time t is described by the tuple $(N(t), A(t), \mathbf{R}(t), \mathbf{C}(t), \mathbf{S}(t))$. We notice that the state space grows exponentially with the cell population size, similarly to the model of electron transfer in Sec. III. However, the analysis of state dynamics above highlights that $(N(t), A(t), R_{\text{TOT}}(t), C_{\text{TOT}}(t), S_{\text{TOT}}(t))$ is a Markov chain, hence complexity reduction can be achieved. Indeed, this stochastic model and such Markov property can be exploited to infer the overall QS dynamics, rather than tracking the dynamics of each specific cell, *i.e.*,

$$p_t(n, a, r, c, s) \triangleq \mathbb{P}(N(t)=n, A(t)=a, R_{\text{TOT}}(t)=r, C_{\text{TOT}}(t)=c, S_{\text{TOT}}(t)=s). \quad (16)$$

V. SIMULATIONS RESULTS

In this section, we present simulation results for the homogeneous cell colony considered in Sec. IV. The parameters are listed in Table I. We consider two different setups: *open system* and *closed system*, both starting from one single cell with initial state $(N(0), A(0), R_{\text{TOT}}(0), C_{\text{TOT}}(0), S_{\text{TOT}}(0)) = (1, 0, 0, 0, 0)$.

a) Open system: In the open system setting, autoinducers may leak and the cell colony grows in an open space. The autoinducer leakage parameters are set to $\xi_{L,1} = 5000$ and $\xi_{L,2} = 0.1$.

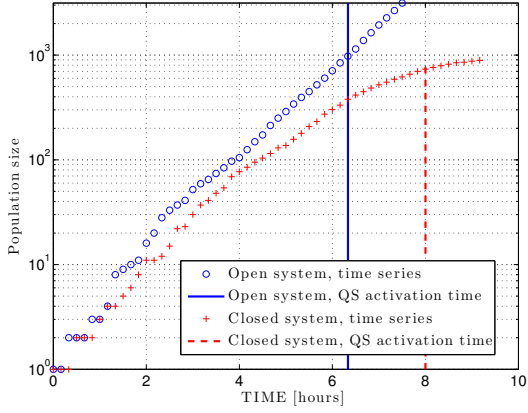
TABLE I
SIMULATION PARAMETERS (nM DENOTES NANOMOLAR CONCENTRATION)

Parameter	Explanation	Value [all of them per hour]	Reference
ρ_{\max}	Maximum duplication rate	1 [per cell]	
ϕ_{cell}	Cell volume	1 [fL]	
β	Autoinducer generation rate	18 [per synthase]	[78]
ξ_D	Autoinducer degradation rate	0.01 [per autoinducer]	[79]
$\eta_{A,th}$	Autoinducer concentration threshold	21.4 [nM]	calculated from [78]
$\epsilon_{0,2}$	Basal receptor generation rate	80 [per cell]	calculated from [78]
$\epsilon_{C,2}$	Activated receptor generation rate	3 [per complex]	calculated from [78]
δ_R	Receptor degradation rate	12 [per receptor]	[80]
γ	Complex generation rate	3.5 [per nM receptor & autoinducer concentrations, per fL]	[80]
δ_C	Complex degradation rate	1.4 [per complex]	[80]
ν_C	Unbinding of complexes	60 [per complex]	[80]
$\epsilon_{0,1}$	Basal synthase generation rate	80 [per cell]	calculated from [78]
$\epsilon_{C,1}$	Activated synthase generation rate	3 [per complex]	calculated from [78]
δ_S	Synthase degradation rate	1 [per synthase]	[81]

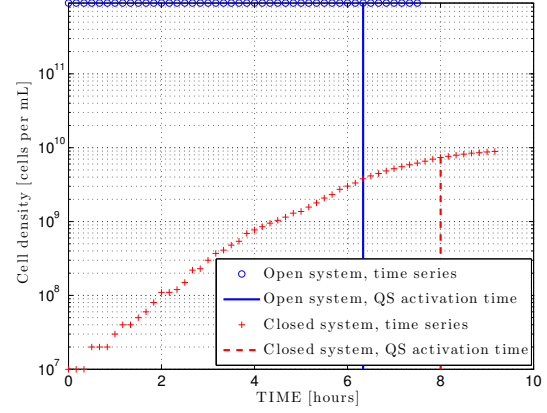
We assume that the cell colony grows in such a way that cells are tightly packed together, and let $\phi_{ex} = 1.1\phi_{cell}$, so that the extracellular environment takes only 10% of the cell volume. The maximum population size is $N_{\max} = \infty$, so that cell growth does not slow down.

b) Closed system: In the closed system setting, autoinducers do not leak ($\xi_{L,1} = \xi_{L,2} = 0$). The cell colony grows in a closed space of volume $V_{tot}(n) = 0.1nL$. We assume that the maximum population size is $N_{\max} = 1000$. With this value, when the population size is maximum the cell volume takes 1% of the total volume.

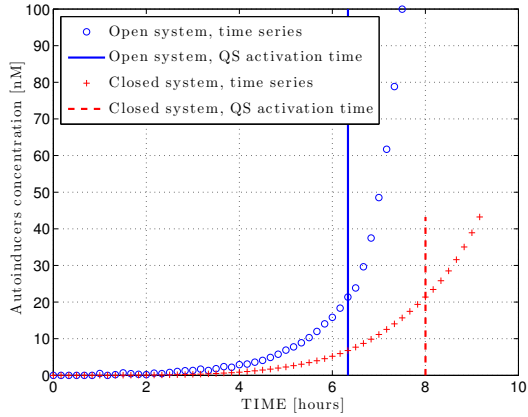
We use Gillespie's exact stochastic simulation algorithm (SSA) [82] to simulate the dynamics of the cell colony. In Figs. 7.a-f, we plot the time series of colony size, cell concentration, the concentration of autoinducers, receptors, complexes and synthases, respectively. In the open system, QS activation occurs after approximately 6 hours, whereas in the closed system QS activation occurs after 8 hours, when the cell population approaches its maximum size and growth starts to slow down (Figs. 7.a-b). The reason is that in the open system a much higher cell density is achieved (Fig. 7.b), resulting in a steeper rise of autoinducer concentration, and thus earlier QS activation, despite the fact that autoinducers leak in the open system. In both cases, after QS activation, complexes start to get formed (Fig. 7.e). Due to the large number of complexes binding to the DNA sites, synthases also build up in the system (Fig. 7.f). As a consequence, the number of autoinducers in the environment builds up faster (Fig. 7.c). In turn, autoinducers and receptors bind more frequently to form complexes, thus activating a positive feedback loop of formation of autoinducer-receptor complexes.



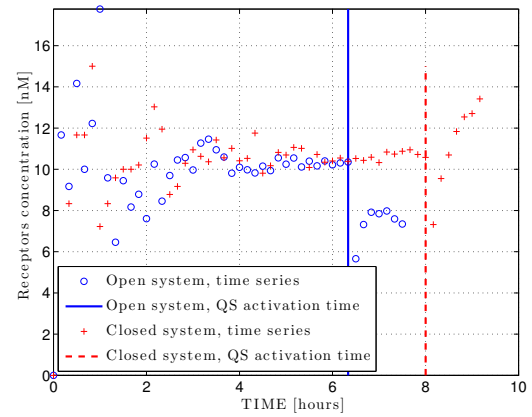
(a) Colony size vs time.



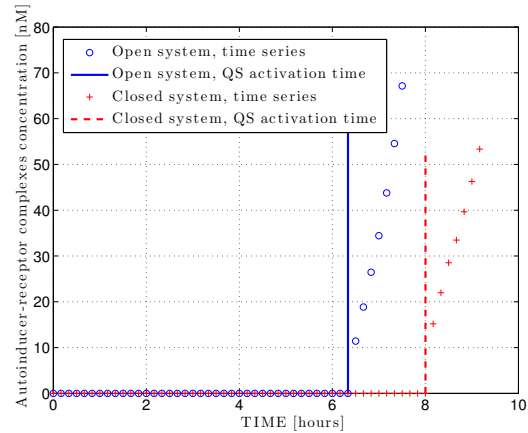
(b) Cell concentration vs time.



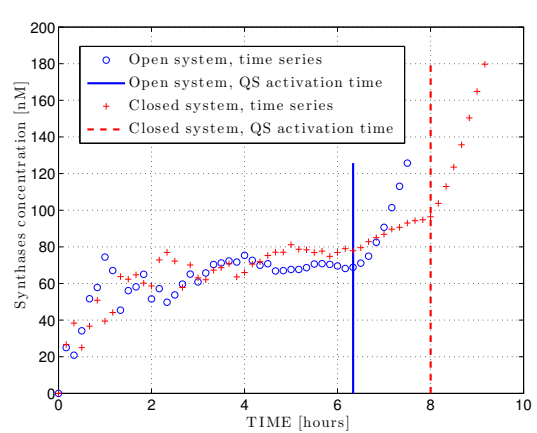
(c) Autoinducers concentration vs time.



(d) Receptors concentration vs time.



(e) Autoinducer-receptor complexes concentration vs time.



(f) Synthases concentration vs time.

Fig. 7. Simulation of QS system. Comparison of open and closed systems. Sampling period 10m.

VI. EXTENSIONS

A. Signal Integration

Our proposed model can be extended to include several aspects of QS observed in nature. Indeed, most QS signaling systems are more complex than the scenario considered in Sec. IV, which includes one receptor-autoinducer pair only. For instance, *Pseudomonas aeruginosa* contains multiple QS networks that work together to monitor changes in the local population of cells. Since the initial discovery of the LasI/LasR system, two other QS circuits in *Pseudomonas aeruginosa* have been discovered and characterized, the RhlI/RhlR and PQS [83]. Recently a fourth IQS QS system has been identified [84]. Although each of these networks has a unique signal and receptor, these four systems are coupled in a feedback network in which each signaling pair regulates the production of both the synthase and receptor of at least one other network. *Vibrio* species have similar complexity in their QS networks [85], integrating information from multiple signals to direct regulatory decisions.

B. Interference

In addition to individual microbes producing multiple signals, QS systems also mediate communication between different species. Many bacteria find themselves in diverse and crowded environments, and many of these neighboring species will also produce autoinducers. The type of autoinducer produced by many *Vibrio* and *Pseudomonas* species has been identified in more than 70 different species [86], and there are examples of signals or enzymes that inhibit QS activation [87]. Within these multispecies communities, there is significant potential for interference with the process of QS activation, *i.e.*, any process which alters the ability of cells to produce, exchange, recognize, or respond to a QS autoinducer. Several mechanisms of QS interference that occur naturally have been identified.

- 1) *Signal synthesis inhibition*: Although no examples of this interaction have been found in nature, a synthetic compound that prevented acyl-homoserine lacone (HSL) production by the TofI synthase in the soil microbe *Burkholderia glumae* has been identified [88]. The inhibitor was found to occupy the active site of the synthase, preventing autoinducer production.
- 2) *Destruction or chemical modification of the autoinducer*: The common example of signal destruction is the AiiA enzyme isolated from *Bacillus* [87]. AiiA is an enzyme that

degrades a common type of autoinducer, thereby preventing the autoinducer from binding to the receptor. In another example, the oxidoreductase from *Burkholderia* is also capable of inactivating some autoinducers through chemical modification, thereby altering the specificity for receptor molecules.

- 3) *Competitive binding to the receptor*: Some species have been shown to produce small molecules that interfere with autoinducer binding to the receptor, for example a furanone compound produced by the alga *Deisea pulchra* [89]. In other cases the competition is from analogous autoinducers. There are many versions of the autoinducer HSL, with differing carbon tails, and each bacteria produces one or more types of HSL. For example, *Pseudomonas aeruginosa* produces the autoinducers C4-HSL and 3oxo-C12-HSL, whereas *Chromobacter violaceum* produces C6-HSL [90]. The receptor of *Chromobacter violaceum* has been found to be activated by C6-HSL, but deactivated or inhibited by HSL with longer carbon tails, such as 3oxo-C12-HSL [91]. In this way, crosstalk between autoinducers produced by neighboring bacteria can influence on signal transduction and QS activation.

Our model in Sec. IV can be extended to include different types of interference. Consider an interfering signal with concentration $\eta_I(t) \triangleq I(t)/V_{tot}(N(t))$, where $I(t)$ is the total amount of interfering molecules in the volume of interest. The interfering signal is injected in the system with rate μ_I , and leaks with rate $\delta_I(N(t))$, which is a function of the colony size, similarly to autoinducers. We may consider the following models of interference:

- *Receptor inhibition*: the interfering signal binds with the receptors, thus competing with the autoinducer signal; unlike the autoinducer-receptor complex, which induces specific gene expression by binding to the DNA sites, the complex formed by the interfering signal and the receptor becomes inactive; the binding of interfering molecules to receptors is a Poisson process with intensity γ_{IR} [per unit of interfering signal and receptor concentrations, per unit volume, per hour]. Since the concentrations of the interfering signal and of free receptors is $\eta_I(t)$ and $\eta_R(t)$, respectively, the overall binding rate is $\gamma_{IR}\eta_I(t)\eta_R(t)V_{cell}(N(t))$, since these reactions occur inside the cells and the total cell volume is $V_{cell}(N(t))$; correspondingly, both $R_{TOT}(t)$ and $I(t)$ decrease by one unit;
- *Synthase blocking*: the interfering signal binds with the active site of the synthase, thus preventing autoinducer production; the binding of interfering molecules to synthases is a

Poisson process with intensity γ_{IS} [per unit of interfering signal and synthase concentrations, per unit volume, per hour]. Since the concentrations of the interfering signal and of synthases is $\eta_I(t)$ and $\eta_S(t)$, respectively, the overall binding rate is $\gamma_{IS}\eta_I(t)\eta_S(t)V_{cell}(N(t))$; correspondingly, both $S_{TOT}(t)$ and $I(t)$ decrease by one unit;

- *Autoinducer degradation*: the interfering signal destroys or chemically modifies the autoinducer signal, thus preventing it from binding to the receptor; the binding of interfering molecules to autoinducers is a Poisson process with intensity δ_{IA} [per unit of interfering signal and autoinducer concentrations, per unit volume, per hour]. Since the concentrations of the interfering signal and of autoinducers is $\eta_I(t)$ and $\eta_A(t)$, respectively, and these reactions occur over the volume $V_{tot}(N(t))$ occupied by the cell colony, the overall binding rate is $\delta_{IA}\eta_I(t)\eta_A(t)V_{tot}(N(t))$; correspondingly, both $A(t)$ and $I(t)$ decrease by one unit; this type of interference can be also represented as an additional source of leakage for the autoinducers, so that their overall leakage rate is $[\delta_A(N(t)) + \delta_{IA}\eta_I(t)]A(t)$.

The model can be extended to include multiple interfering signals in a similar fashion.

VII. CONCLUSIONS

In this position paper, we have explored how abstractions from communications, networking and information theory can play a role in understanding and modeling bacterial interactions. In particular, we have examined two forms of interactions in bacterial systems: *electron transfer* and *quorum sensing*. We have presented a stochastic queuing model of electron transfer for a single cell, and we have showed how the proposed single-cell model can be extended to bacterial cables, by allowing for electron transfer between neighboring cells. We have performed a capacity analysis for a bacterial cable, demonstrating that such model is amenable to complexity reduction. Moreover, we have provided a new queuing model for quorum sensing, which captures the dynamics of the quorum sensing signaling system, signal interactions, and cell duplication within a stochastic framework. We have shown that sufficient statistics can be identified, which allow a compact state space representation, and we have provided preliminary simulation results. Our investigation reveals that queuing models effectively capture interactions in microbial communities and the inherent randomness exhibited by cell colonies in nature, and they are amenable to complexity reduction using methods based on statistical physics and

wireless network design. Thus, they represent powerful predictive tools, which will aid the design of systems exploiting bacterial capabilities.

REFERENCES

- [1] A. J. Kaufman, “Early earth: Cyanobacteria at work,” *Nature Geoscience*, vol. 7, no. 4, pp. 253–254, 04 2014. [Online]. Available: <http://dx.doi.org/10.1038/ngeo2128>
- [2] C. M. Hogan, “Bacteria,” *Encyclopedia of Earth. Washington DC: National Council for Science and the Environment*, 2010.
- [3] G. A. Kowalchuk, S. E. Jones, and L. L. Blackall, “Commentary: Microbes orchestrate life on earth,” *ISME Journal*, vol. 2, pp. 795–796, 2008.
- [4] G. Reguera, K. D. McCarthy, T. Mehta, J. S. Nicoll, M. T. Tuominen, and D. R. Lovley, “Extracellular electron transfer via microbial nanowires,” *Nature*, vol. 435(7045), pp. 1098–1101, 2005.
- [5] C. Pfeffer *et al.*, “Filamentous bacteria transport electrons over centimetre distances,” *Nature*, vol. 491(7423), pp. 218–221, 2012.
- [6] M. B. Miller and B. L. Bassler, “Quorum sensing in bacteria,” *Annual Review of Microbiology*, vol. 55, no. 1, pp. 165–199, 2001.
- [7] K. L. Visick and C. Fuqua, “Decoding Microbial Chatter: Cell-Cell Communication in Bacteria,” *Journal of Bacteriology*, vol. 187, no. 16, pp. 5507–5519, 2005. [Online]. Available: <http://jlb.asm.org/content/187/16/5507.short>
- [8] K. Nealson, T. Platt, and J. Hastings, “Cellular Control of Synthesis and Activity of Bacterial Luminescent System,” *Journal of Bacteriology*, vol. 104, no. 1, pp. 313–322, 1970.
- [9] T. Nakano, A. W. Eckford, and T. Haraguchi, *Molecular communication*. Cambridge University Press, 2013.
- [10] I. Mian and C. Rose, “Communication theory and multicellular biology,” *Integrative Biology*, vol. 3, no. 4, pp. 350–367, 2011.
- [11] M. Y. El-Naggar and S. E. Finkel, “Live Wires: Electrical Signaling Between Bacteria,” *The Scientist*, vol. 27, no. 5, pp. 38–43, 2013.
- [12] S. Kato, K. Hashimoto, and K. Watanabe, “Microbial interspecies electron transfer via electric currents through conductive minerals,” *Proceedings of the National Academy of Sciences*, vol. 109, no. 25, pp. 10 042–10 046, June 2012.
- [13] S. Pirbadian and M. Y. El-Naggar, “Multistep hopping and extracellular charge transfer in microbial redox chains,” *Physical Chemistry Chemical Physics*, vol. 14, pp. 13 802–13 808, 2012.
- [14] C. A. Desoer, “Communication through channels in cascade,” Ph.D. dissertation, Massachusetts Institute of Technology, 1953.
- [15] R. Silverman *et al.*, “On binary channels and their cascades,” *IRE Transactions on Information Theory*, vol. 1, no. 3, pp. 19–27, 1955.
- [16] H. Goldman and R. Sommer, “An analysis of cascaded binary communication links,” *IRE Transactions on Communications Systems*, vol. 10, no. 3, pp. 291–299, 1962.
- [17] M. Simon, “On the capacity of a cascade of identical discrete memoryless nonsingular channels,” *IEEE Transactions on Information Theory*, vol. 16, no. 1, pp. 100–102, Jan 1970.
- [18] T. M. Cover and J. A. Thomas, *Elements of Information Theory*. New York, NY, USA: Wiley-Interscience, 1991.
- [19] A. Einolghozati, M. Sardari, and F. Fekri, “Relaying in diffusion-based molecular communication,” in *IEEE International Symposium on Information Theory Proceedings (ISIT)*. IEEE, 2013, pp. 1844–1848.

- [20] M. Ş. Kuran, H. B. Yilmaz, T. Tugcu, and I. F. Akyildiz, "Interference effects on modulation techniques in diffusion based nanonetworks," *Nano Communication Networks*, vol. 3, no. 1, pp. 65–73, 2012.
- [21] H. Arjmandi, A. Gohari, M. N. Kenari, and F. Bateni, "Diffusion-based nanonetworking: A new modulation technique and performance analysis," *IEEE Communications Letters*, vol. 17, no. 4, pp. 645–648, 2013.
- [22] R. Mosayebi, H. Arjmandi, A. Gohari, M. Nasiri-Kenari, and U. Mitra, "Receivers for diffusion-based molecular communication: Exploiting memory and sampling rate," *IEEE Journal on Selected Areas in Communications*, vol. 32, no. 12, pp. 2368–2380, 2014.
- [23] A. Noel, K. C. Cheung, and R. Schober, "Optimal receiver design for diffusive molecular communication with flow and additive noise," *IEEE Transactions on NanoBioscience*, vol. 13, no. 3, pp. 350–362, 2014.
- [24] M. Pierobon and I. F. Akyildiz, "A physical end-to-end model for molecular communication in nanonetworks," *IEEE Journal on Selected Areas in Communications*, vol. 28, no. 4, pp. 602–611, 2010.
- [25] K. Srinivas, A. W. Eckford, and R. S. Adve, "Molecular communication in fluid media: The additive inverse gaussian noise channel," *IEEE Transactions on Information Theory*, vol. 58, no. 7, pp. 4678–4692, 2012.
- [26] H. Li, S. M. Moser, and D. Guo, "Capacity of the memoryless additive inverse gaussian noise channel," *IEEE Journal on Selected Areas in Communications*, vol. 32, no. 12, pp. 2315–2329, 2014.
- [27] A. Einolghozati, M. Sardari, and F. Fekri, "Design and analysis of wireless communication systems using diffusion-based molecular communication among bacteria," *IEEE Transactions on Wireless Communications*, vol. 12, no. 12, pp. 6096–6105, 2013.
- [28] A. Einolghozati, M. Sardari, A. Beirami, and F. Fekri, "Capacity of discrete molecular diffusion channels," in *IEEE International Symposium on Information Theory Proceedings (ISIT)*. IEEE, 2011, pp. 723–727.
- [29] M. Pierobon and I. F. Akyildiz, "Capacity of a diffusion-based molecular communication system with channel memory and molecular noise," *IEEE Transactions on Information Theory*, vol. 59, no. 2, pp. 942–954, 2013.
- [30] C. E. Shannon *et al.*, "Two-way communication channels," in *Proc. 4th Berkeley Symp. Math. Stat. Prob.*, vol. 1, 1961, pp. 611–644.
- [31] E. C. Van Der Meulen, "The discrete memoryless channel with two senders and one receiver," in *Proc. IEEE Int. Symp. Information Theory (ISIT)*, 1971, p. 78.
- [32] H. H.-J. Liao, "Multiple access channels." DTIC Document, Tech. Rep., 1972.
- [33] R. Ahlswede, "The capacity region of a channel with two senders and two receivers," *The Annals of Probability*, pp. 805–814, 1974.
- [34] T. M. Cover, "Broadcast channels," *IEEE Transactions on Information Theory*, vol. 18, no. 1, pp. 2–14, 1972.
- [35] —, "Comments on broadcast channels," *IEEE Transactions on information theory*, vol. 44, no. 6, pp. 2524–2530, 1998.
- [36] A. Einolghozati, M. Sardari, A. Beirami, and F. Fekri, "Consensus problem under diffusion-based molecular communication," in *45th Annual Conference on Information Sciences and Systems (CISS)*. IEEE, 2011, pp. 1–6.
- [37] T. Vicsek, A. Czirók, E. Ben-Jacob, I. Cohen, and O. Shochet, "Novel type of phase transition in a system of self-driven particles," *Phys. Rev. Lett.*, vol. 75, pp. 1226–1229, Aug 1995. [Online]. Available: <http://link.aps.org/doi/10.1103/PhysRevLett.75.1226>
- [38] T. Vicsek and A. Zafeiris, "Collective motion," *Physics Reports*, no. 0, 2012.
- [39] H.-S. Song, W. R. Cannon, A. S. Beliaev, and A. Konopka, "Mathematical modeling of microbial community dynamics: A methodological review," *Processes*, vol. 2, no. 4, pp. 711–752, 2014. [Online]. Available: <http://www.mdpi.com/2227-9717/2/4/711>

- [40] P. Mina, M. di Bernardo, N. J. Savery, and K. Tsaneva-Atanasova, “Modelling emergence of oscillations in communicating bacteria: a structured approach from one to many cells,” *Journal of The Royal Society Interface*, vol. 10, no. 78, 2012.
- [41] A. M. Ardekani and E. Gore, “Emergence of a limit cycle for swimming microorganisms in a vortical flow of a viscoelastic fluid,” *Phys. Rev. E*, vol. 85, p. 056309, May 2012. [Online]. Available: <http://link.aps.org/doi/10.1103/PhysRevE.85.056309>
- [42] R. E. Baker, C. A. Yates, and R. Erban, “From microscopic to macroscopic descriptions of cell migration on growing domains,” *Bulletin of mathematical biology*, vol. 72, no. 3, pp. 719–762, 2010.
- [43] I. Klapper and J. Dockery, “Mathematical description of microbial biofilms,” *SIAM Review*, vol. 52, no. 2, pp. 221–265, 2010. [Online]. Available: <http://dblp.uni-trier.de/db/journals/siamrev/siamrev52.html#KlapperD10>
- [44] N. Bellomo and J. Soler, “On the mathematical theory of the dynamics of swarms viewed as complex systems,” *Mathematical Models and Methods in Applied Sciences*, vol. 22, no. supp01, p. 1140006, 2012. [Online]. Available: <http://www.worldscientific.com/doi/abs/10.1142/S0218202511400069>
- [45] J. F. Hammond, E. J. Stewart, J. G. Younger, M. J. Solomon, and D. M. Bortz, “Spatially heterogeneous biofilm simulations using an immersed boundary method with lagrangian nodes defined by bacterial locations,” *CoRR*, vol. abs/1302.3663, 2013. [Online]. Available: <http://dblp.uni-trier.de/db/journals/corr/corr1302.html#abs-1302-3663>
- [46] A. Friedman, B. Hu, and C. Xue, “On a multiphase multicomponent model of biofilm growth,” *Archive for Rational Mechanics and Analysis*, vol. 211, no. 1, pp. 257–300, 2014. [Online]. Available: <http://dx.doi.org/10.1007/s00205-013-0665-1>
- [47] C. A. Yates, R. Baker, R. Erban, and P. Maini, “Refining self-propelled particle models for collective behaviour,” *Canadian Applied Maths Quarterly (CAMQ)*, vol. 18, no. 3, 2011.
- [48] C. Waltermann and E. Klipp, “Information theory based approaches to cellular signaling,” *Biochimica et Biophysica Acta (BBA)-General Subjects*, vol. 1810, no. 10, pp. 924–932, 2011.
- [49] P. Mehta, S. Goyal, T. Long, B. L. Bassler, and N. S. Wingreen, “Information processing and signal integration in bacterial quorum sensing,” *Molecular systems biology*, vol. 5, no. 1, p. 325, 2009.
- [50] R. Cheong, A. Rhee, C. J. Wang, I. Nemenman, and A. Levchenko, “Information transduction capacity of noisy biochemical signaling networks,” *science*, vol. 334, no. 6054, pp. 354–358, 2011.
- [51] P. D. Pérez, J. T. Weiss, and S. J. Hagen, “Noise and crosstalk in two quorum-sensing inputs of vibrio fischeri,” *BMC systems biology*, vol. 5, no. 1, p. 153, 2011.
- [52] U. Mitra, N. Michelusi, S. Pirbadian, H. Koorehdavoudi, M. El-Nagggar, and P. Bogdan, “Queueing theory as a modeling tool for Bacterial Interaction: Implications for Microbial Fuel Cells,” in *International Conference on Computing, Networking and Communications (ICNC)*, February 16-19, 2015, Anaheim, CA, USA.
- [53] M. Levorato, U. Mitra, and A. Goldsmith, “Structure-based learning in wireless networks via sparse approximation,” *EURASIP Journal on Wireless Communications and Networking*, vol. 1, pp. 1–15, 2012, invited paper.
- [54] K. Rabaey and R. A. Rozendal, “Microbial electrosynthesis – revisiting the electrical route for microbial production,” *Nature Reviews Microbiology*, vol. 8, no. 10, pp. 706–716, 2010.
- [55] B. E. Logan, “Exoelectrogenic bacteria that power microbial fuel cells,” *Nature Reviews Microbiology*, vol. 7, no. 5, pp. 375–381, 2009.
- [56] H. J. Kim, H. S. Park, M. Hyun, I. S. Chang, M. Kim, and B. Kim, “A mediator-less microbial fuel cell using a metal reducing bacterium, *Shewanella putrefaciens*,” *Enzyme and Microbial Technology*, vol. 30, no. 2, pp. 145–152, 2002.
- [57] J. S. McLean, G. Wanger, Y. A. Gorby, M. Wainstein, J. McQuaid, S. Ishii, O. Bretschger, H. Beyenal, and K. H. Nealson,

- “Quantification of electron transfer rates to a solid phase electron acceptor through the stages of biofilm formation from single cells to multicellular communities,” *Environmental science & technology*, vol. 44, no. 7, pp. 2721–2727, 2010.
- [58] M. Gambello and B. Iglewski, “Cloning and characterization of the *Pseudomonas aeruginosa* lasR gene, a transcriptional activator of elastase expression,” *Journal of Bacteriology*, vol. 173, pp. 3000–3009, 1991.
- [59] P. Singh, A. Schaefer, M. Parsek, T. Moninger, M. Welsh, and E. Greenberg, “Quorum-sensing signals indicate that cystic fibrosis lungs are infected with bacterial biofilms,” *Nature*, vol. 407, pp. 762–764, Oct. 2000.
- [60] D. Erickson, R. Endersby, A. Kirkham, K. Stuber, D. Vollman, H. Rabin, I. Mitchell, and D. Storey, “*Pseudomonas aeruginosa* quorum-sensing systems may control virulence factor expression in the lungs of patients with cystic fibrosis,” *Infection and Immunity*, vol. 70, pp. 1783–1790, 2002.
- [61] K. Rumbaugh, J. Griswold, B. Iglewski, and A. Hamood, “Contribution of quorum sensing to the virulence of *Pseudomonas aeruginosa* in burn wound infections,” *Infection and Immunity*, vol. 67, pp. 5854–5862, 1999.
- [62] T. Rasmussen and M. Givskov, “Quorum-sensing inhibitors as anti-pathogenic drugs,” *International Journal of Medical Microbiology*, vol. 296, pp. 149–161, 2006.
- [63] R. Allen, R. Popat, S. Diggle, and S. Brown, “Targeting virulence: can we make evolution-proof drugs?” *Nature Reviews Microbiology*, vol. 12, pp. 300–308, 2014.
- [64] V. Kalia, “Quorum sensing inhibitors: An overview,” *Biotechnology Advances*, vol. 31, pp. 224–245, 2013.
- [65] N. Lane, “Why Are Cells Powered by Proton Gradients?” *Nature Education*, vol. 3(9):18, 2010.
- [66] N. Michelusi, S. Pirbadian, M. El-Naggar, and U. Mitra, “A Stochastic Model for Electron Transfer in Bacterial Cables,” *IEEE Journal on Selected Areas in Communications*, vol. 32, no. 12, pp. 2402–2416, Dec. 2014.
- [67] V. Ozalp, P. T.R., N. L.J., and O. L.F., “Time-resolved measurements of intracellular ATP in the yeast *Saccharomyces cerevisiae* using a new type of nanobiosensor,” *Journal of Biological Chemistry*, pp. 37 579–37 588, Nov. 2010.
- [68] W. Smith and J. Hashemi, *Foundations of Materials Science and Engineering*, ser. McGraw-Hill series in materials science and engineering. McGraw-Hill, 2003.
- [69] N. Michelusi and U. Mitra, “Capacity of electron-based communication over bacterial cables: the full-CSI case,” *IEEE Transactions on Molecular, Biological and Multi-Scale Communications*, 2015, to appear.
- [70] F. J. Meysman, N. Risgaard-Petersen, S. Y. Malkin, and L. P. Nielsen, “The geochemical fingerprint of microbial long-distance electron transport in the seafloor,” *Geochimica et Cosmochimica Acta*, vol. 152, no. 0, pp. 122–142, 2015. [Online]. Available: <http://www.sciencedirect.com/science/article/pii/S0016703714007236>
- [71] J. Chen and T. Berger, “The capacity of finite-State Markov Channels with feedback,” *IEEE Transactions on Information Theory*, vol. 51, no. 3, pp. 780–798, March 2005.
- [72] D. Bertsekas, *Dynamic programming and optimal control*. Athena Scientific, Belmont, Massachusetts, 2005.
- [73] D. L. Stauff and B. L. Bassler, “Quorum Sensing in *Chromobacterium violaceum*: DNA Recognition and Gene Regulation by the CviR Receptor,” *Journal of Bacteriology*, vol. 193, no. 15, pp. 3871–3878, Aug. 2011.
- [74] E. Stewart, R. Madden, G. Paul, and F. Taddei, “Aging and death in an organism that reproduces by morphologically symmetric division,” *PLoS Biology*, vol. 3, no. 2, Feb. 2005.
- [75] C. J. Kastrup, F. Shen, and R. F. Ismagilov, “Response to Shape Emerges in a Complex Biochemical Network and Its Simple Chemical Analogue,” *Angewandte Chemie International Edition*, vol. 46, no. 20, pp. 3660–3662, 2007. [Online]. Available: <http://dx.doi.org/10.1002/anie.200604995>
- [76] K. Gray and J. R. Garey, “The evolution of bacterial LuxI and LuxR quorum sensing regulators,” *Microbiology*, vol. 147, no. 8, pp. 2379–2387, Aug. 2001.

- [77] S.-W. Teng, Y. Wang, K. Tu, T. Long, P. Mehta, N. S. Wingreen, B. L. Bassler, and N. Ong, "Measurement of the Copy Number of the Master Quorum-Sensing Regulator of a Bacterial Cell," *Biophysical Journal*, vol. 98, no. 9, pp. 2024–2031, May 2010.
- [78] J. Perez-Velazquez, B. Quinones, B. A. Hense, and C. Kuttler, "A mathematical model to investigate quorum sensing regulation and its heterogeneity in *Pseudomonas syringae* on leaves," *Ecological Complexity*, vol. 21, pp. 128–141, 2015. [Online]. Available: <http://www.sciencedirect.com/science/article/pii/S1476945X1400155X>
- [79] J. R. Chandler, S. Heilmann, J. E. Mittler, and E. P. Greenberg, "Acyl-homoserine lactone-dependent eavesdropping promotes competition in a laboratory co-culture model," *ISME Journal*, vol. 6, no. 12, pp. 2219–2228, 12 2012. [Online]. Available: <http://dx.doi.org/10.1038/ismej.2012.69>
- [80] C. Smith, H. Song, and L. You, "Signal discrimination by differential regulation of protein stability in quorum sensing," *Journal of Molecular Biology*, no. 382, pp. 1290–1297, Oct. 2008.
- [81] Bionumbers. [Online]. Available: <http://bionumbers.hms.harvard.edu>
- [82] D. T. Gillespie, "Exact stochastic simulation of coupled chemical reactions," *J. Physical Chemistry*, vol. 81, no. 25, pp. 2340–2361, Dec. 1977. [Online]. Available: <http://dx.doi.org/10.1021/j100540a008>
- [83] P. Jimenez, G. Koch, J. A. Thompson, K. B. Xavier, R. H. Cool, and W. J. Quax, "The Multiple Signaling Systems Regulating Virulence in *Pseudomonas aeruginosa*," *Microbiology and Molecular Biology Reviews*, vol. 76, no. 1, pp. 46–65, March 2012.
- [84] J. Lee, J. Wu, Y. Deng, J. Wang, C. Wang, J. Wang, C. Chang, Y. Dong, P. Williams, and L. Zhang, "A cell-cell communication signal integrates quorum sensing and stress response," *Nature Chemical Biology*, vol. 9, no. 5, pp. 339–343, Mar. 2013.
- [85] S. Teng, J. Schaffer, K. Tu, P. Mehta, W. Lu, N. Ong, B. Bassler, and N. Wingreen, "Active regulation of receptor ratios controls integration of quorum-sensing signals in *Vibrio harveyi*," *Molecular Systems Biology*, vol. 7, no. 491, May 2011.
- [86] N. Kimura, "Metagenomic approaches to understanding phylogenetic diversity in quorum sensing," *Virulence*, vol. 5, no. 3, pp. 433–442, Apr. 2014.
- [87] G. Rampioni, L. Leoni, and P. Williams, "The art of antibacterial warfare: Deception through interference with quorum sensing-mediated communication," *Bioorganic Chemistry*, vol. 55, no. 0, pp. 60 – 68, 2014, bio-Organic Chemistry of Antibacterial Drug Discovery. [Online]. Available: <http://www.sciencedirect.com/science/article/pii/S0045206814000297>
- [88] K.-G. Chan, S. Atkinson, K. Mathee, C.-K. Sam, S. R. Chhabra, M. Camara, C.-L. Koh, and P. Williams, "Characterization of N-acylhomoserine lactone-degrading bacteria associated with the *Zingiber officinale* (ginger) rhizosphere: Co-existence of quorum quenching and quorum sensing in *Acinetobacter* and *Burkholderia*," *BMC Microbiology*, vol. 11, no. 51, 2011.
- [89] J. E. Gonzalez and N. D. Keshavan, "Messing with Bacterial Quorum Sensing," *Microbiology and Molecular Biology Reviews*, vol. 70, no. 4, p. 859–875, Dec. 2006.
- [90] P. Williams, K. Winzer, W. Chan, and M. Camara, "Look who's talking: communication and quorum sensing in the bacterial world," *Philosophical Transactions of the Royal Society B: Biological Sciences*, vol. 362, no. 1483, pp. 1119–1134, July 2007.
- [91] K. McClean, M. Winson, L. Fish, A. Taylor, S. Chhabra, M. Camara, M. Daykin, J. Lamb, S. Swift, B. Bycroft, G. Stewart, and P. Williams, "Quorum sensing and *Chromobacterium violaceum*: exploitation of violacein production and inhibition for the detection of N-acylhomoserine lactones," *Microbiology*, vol. 143, no. 12, pp. 3703–3711, Dec. 1997.